Final Report

Cover Page

Company Name and Address: Particle Beam Lasers, Inc.
18925 Dearborn Street
Northridge, CA 91324-2807

Principal Investigator: Robert J. Weggel

Project Title: HTS Solenoid for Neutron Scattering

Topic No: 17 Instrumentation and Tools for Materials Research using Neutron Scattering

Subtopic: (a) Advanced Sample Environments

Proprietary data legend:

Sentences, paragraphs, tables, charts, and other graphics containing trade secrets, commercial, and/or financial information are marked with brackets [ ].

Identification and Significance of the Problem or Opportunity, and Technical Approach

Neutron scattering experiments would benefit from magnets with fields at least 50% more intense than the ~17 T presently available from conventional low-temperature superconductors (LTS). A high temperature superconductor (HTS) such as ReBCO, operating at ~4 K as a **high field** superconductor, is essential, because LTS falls far short of the needed combination of critical field and critical current density.

To advance magnet technology for neutron-scattering experiments, Particle Beam Lasers, LLC and the Superconducting Magnet Division (SMD) of Brookhaven National Laboratory (BNL) have capitalized upon their expertise and equipment, some of which was developed during SBIR/STTR collaborations, including ones that designed, built and tested the two HTS solenoids of Fig. 1, designed to be capable of nesting to generate a field to reach the desired range.

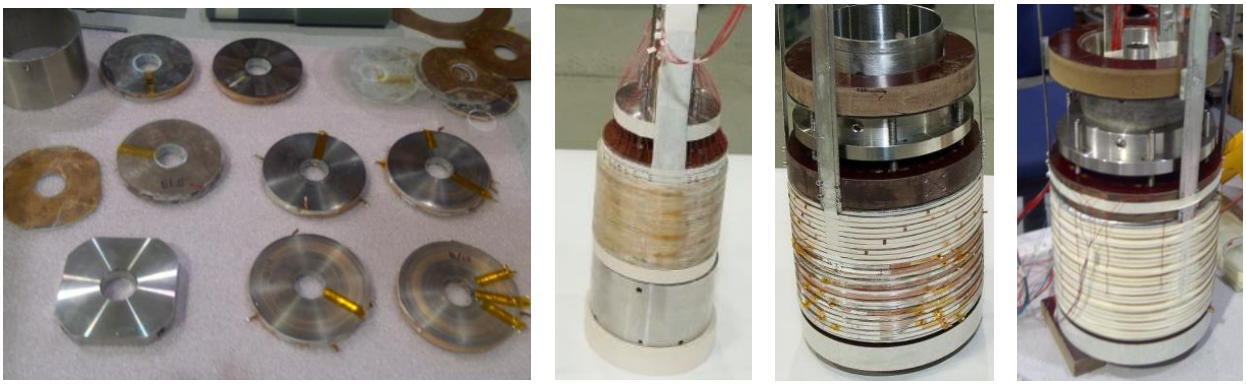

Fig. 1a-d.: High field HTS solenoids designed, built and tested by PBL/BNL collaborations. Left: 25-mm bore pancake coils for insert magnet. Left-center: Solenoid that generated 16 T. Right-center: Solenoid with 12 double-pancakes of 100 mm bore. Right: Nested set.

The inner of these two solenoids, of 25-mm i.d. and 91-mm o.d., operated at a current density greater than 500 A/mm^2 and generated nearly 16 T, a world record in 2013 for a magnet exclusively of HTS. The outer solenoid had respective inner and outer diameters of 100 mm and 163 mm. A half-length version generated more than 6 T (maximum ambient field = 9.2 T). Full length, its designed contribution is 10 T; nested, the pair of solenoids might be capable of 25 T or more. These solenoids employed metallic (stainless steel) insulation; the technology led to further R&D at BNL on HTS magnets. BNL also has tested magnets with conventional insulation and no insulation.

Another valuable legacy of previous PBL/BNL collaborations is the advanced system of Fig. 2, to detect incipient magnet quenches and shut down the magnet to protect it from burnout. Such a system is essential to successful magnet operation.

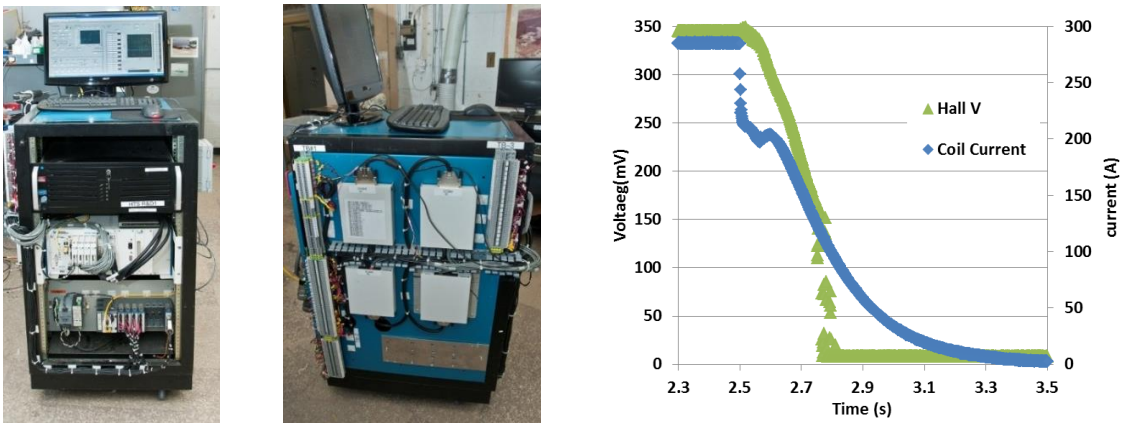

Fig. 2a-c. Quench-detection and magnet-protection system developed during PBL/BNL SBIR/STTR collaborations. Left & center: Hardware (32 channels, 1 kV). Right: Time dependence of magnet's current—and also central field, as measured by Hall voltage—during rapid shutdown. The very rapid drop in current from 285 A to 230 A is from inductive commutation of current to copper discs between the magnet's double pancakes of conductor.

The major experimental accomplishment in Phase I was to utilize conductor on hand at BNL to wind conical coils of ReBCO tape and to test them, not merely at 77 K, as promised in the Proposal, but also at 4 K. The major analytical accomplishment was to generate preliminary designs of 25-T magnets with many nested solenoids, using HTS in all coils that see a field higher than 14 T. Valuable in this endeavor was input from Dr. John Tranquada and Dr. Igor Zaliznyak of BNL, and Dr. Roy I. Cutler of ORNL, all experts in the field of neutron scattering experiments.

Design requirements for high field magnet for neutron scattering

High magnetic field is an important tool for tuning the state of matter, creating new states and quantum phases, and changing the fundamental properties of materials. Magnetic fields can modify transport properties of conductors, correlations in magnetic insulators, and the way conduction electrons interact with atomic moments in magnetic metals. Neutron-scattering techniques provide a powerful tool for studying these atomic, molecular and microscopic properties and correlations in condensed matter systems. The importance of developing high magnetic field environments for such studies has therefore been widely appreciated, e.g., in the National Research Council of the National Academy of Sciences report, "High Magnetic Field Science and Its Application in the United States: Status and Future Directions".[1] Workshops by the ORNL Neutron Science Directorate[2-4] discussed advances in high magnetic field science and practical routes for building high-field magnets for neutron scattering to enable the new science that neutron-scattering measurements in high magnetic fields can provide. A recent Workshop[4] focused on the new opportunities provided by the progress in the commercial development of high-temperature superconductor technology.

Low-temperature superconductor (LTS) magnets for neutron-scattering measurements can reach only ~17 T. To reach 26 T, the dedicated beam line EXED at the Helmholtz Zentrum, Berlin (HZB)[5,6] augmented the field from the superconducting outer coils with 11 teslas from a resistive insert consuming 4.4 MW, at a capital cost of $30 M for the resistive magnet, power supply and cooling system, and also operating costs orders of magnitude greater than for an all-superconducting system.

The magnetic field is horizontal, with a viewing angle of only 30°. The geometry severely limits neutron spectroscopic studies, which require rotation of the sample with respect to the detector array and the incident beam in order to explore its reciprocal space. HTS coils should be able to deliver magnetic fields as intense as 25 T.[4] A 25 T split-coil, vertical-field magnet could be similar in usability and versatility to the LTS systems that are currently the mainstay of neutron scattering studies. Ideally, the magnet would be experiment-friendly, with large viewing ports (~90°-180° horizontally and 5°-15° vertically) and compact and portable between different neutron spectrometers, rather than requiring a dedicated beam line.

Magnet design and requirements

The main requirement for a neutron- or X-ray-scattering magnet is a large solid angle for the passage of incident and scattered beams, unobscured by the magnet coils and their support structures. Especially for time-of-flight (TOF) neutron spectroscopy, the viewing ports should be as free as possible of material, to avoid spurious TOF background features from neutrons scattering in, for example, thin-walled aluminum cylinders separating the members of a split-coil pair.[7-9]

Two basic magnet geometries are used to position the coils out of incident and scattered beam paths in neutron-scattering magnets: (i) vertical-field (VF), split-coil, and (ii) horizontal-field, conical-bore. The latter optionally may split the coil to accommodate the incident beam and/or the top-loading sample environments. The former is used in most high field LTS magnets for neutron scattering; the HZB uses the latter. The horizontal field geometry also is used in some scattering experiments that require the field direction to be paraxial with the incident beam, or to rotate in the horizontal scattering plane. These include some experiments using reflectometry or small-angle neutron scattering (SANS), or that require the field to be quasi-parallel with the momentum transfer vector, which usually is in the horizontal scattering plane. The LTS magnets used for such measurements typically have horizontal-field, conical-bore geometry with an opening up to 90° (±45°) that can be positioned either along, or perpendicular to, the incident beam. For the latter, the coil usually is split to accommodate the incident beam as well as the top-loading sample environments. Horizontal-field magnets typically have fields lower than vertical-field systems, usually no more than 9 T; the recent 17 T SANS magnet[10] has only limited acceptance.

Preferred is the vertical-field, split-coil geometry, which is compatible with the sample rotation techniques for broad surveys of reciprocal space. Furthermore, stray fields at the side of magnets typically are only half that at the same distance along the axis and easier to shield or to mitigate using compensation coils. Additionally, the geometry more easily accommodates ^{3}He and dilution-refrigeration inserts, pressure cells, and high-temperature inserts, providing opportunities for neutron studies under multiple extreme thermodynamic conditions. For these reasons, the recommendation of the Ultra-High Field Magnets for X-Ray and Neutron Scattering Using High Temperature Superconductors Workshop was to concentrate on developing magnets with the vertical-field, split-coil geometry.[4]

Table 1 presents magnet parameters specified in an ORNL solicitation for a magnet of 25 T.

Table I: Illustrative Specs of 25 Tesla Magnet for Diffraction Measurements

Maximum field	25 teslas
Field homogeneity:	< 1.4% over cylinder of 15 mm diameter and length
Stray field (at maximum field)	≤ 0.1 T @ 2 m; ≤ 0.01T @ 4 m
Minimum open bore diameter	40 mm
Minimum coil split height	17 mm
Vertical opening	−5° to +5°, flaring from ±7.5 mm, the ends of the sample
Horizontal opening	4 openings, each 60° (±30°)

Anticipated Public Benefits

A publication[11] by the Institute of Physics states, "Neutron scattering is routinely used in modern science to understand material properties on the atomic scale. Originally developed as a tool for physics, the method has led to advances in many areas of science, from clean energy and the environment, pharmaceuticals and healthcare, through to nanotechnology, materials engineering, fundamental physics and IT. …

"Neutron scattering is used in many different scientific fields. Neutrons can be used to study the dynamics of chemical reactions at interfaces for chemical and biochemical engineering, in food science, drug synthesis and healthcare. Neutrons can probe deep into solid objects such as turbine blades, gas pipelines and welds to give microscopic insight into the strains and stresses that affect the operational lifetimes of crucial engineering components. Neutron studies of nano-particles, low-dimensional systems and magnetism are used for the development of next-generation computer and IT technology, data storage, sensors and superconducting materials. Neutron scattering is a delicate and non-destructive measurement technique, making it ideal for use in heritage science. …

"Neutron scattering can be used to address the global challenges facing society, and to make developments that have immediate or long-term economic impact."

Many consider neutron scattering to be the most valuable of all tools for investigating matter of all sorts, employing thousands of researchers, as evidenced by organizations such as the Neutron Scattering Society of America and the European Neutron Scattering Association. Their research is of extreme commercial as well as intellectual value, justifying the expenditure of billions of dollars on neutron sources and detectors, including magnets such as those from HTS-110, a division of the SCOTT Group.

As with nuclear magnetic resonance, sensitivity and resolution improve **very** greatly with increased magnetic field intensity. The R&D of this SBIR/STTR, to develop the technology to design, fabricate and test proof-of principle and prototype magnets, has the potential to broaden and deepen greatly the value of neutron scattering, carrying it into a new regime of utility. Developing the technology for such magnets is vital for their success, and therefore amply justifies the investment.

PBL/BNL experience in high field HTS solenoid development

PBL and BNL have acquired extensive experience in high field HTS solenoid technology by collaborating on several Phase I and Phase II SBIRs supported by the Office of High Energy Physics. The solenoid of Fig. 1b, consisting of seven double pancakes of 25 mm i.d., generated 16 T, a record field at that time for an all-HTS solenoid. The solenoid of Fig. 1d, with twelve double pancakes of 100 mm bore, designed as an outsert for the inner HTS solenoid, generated, at only half length (Fig. 1c), 6.4 T on-axis and 9.2 T maximum. Both solenoids used insulation of stainless steel.

In addition, as described in the Related Research section below, Dr. Gupta and his BNL team have designed, constructed, and tested many other large high-field HTS magnets, including a solenoid for a superconducting magnetic energy storage (SMES) project. The team led a project to fabricate a 25 T solenoid of 100 mm bore for the Institute for Basic Science (IBS).

PBL consulted distinguished members of the user community as part of the effort. PBL's relationship with scientists at BNL and ORNL provided valuable input on the requirements for the high field magnet we hope to build in Phase II.

Geometry of Illustrative Neutron-Scattering Magnets of Three Designs

Figures 3 and 4 reveal the geometry of three illustrative designs for magnets to generate 25 T for neutron scattering experiments. Figure 3 presents views from above a quadrant of the upper half of each magnet; Figure 4 presents views from below.

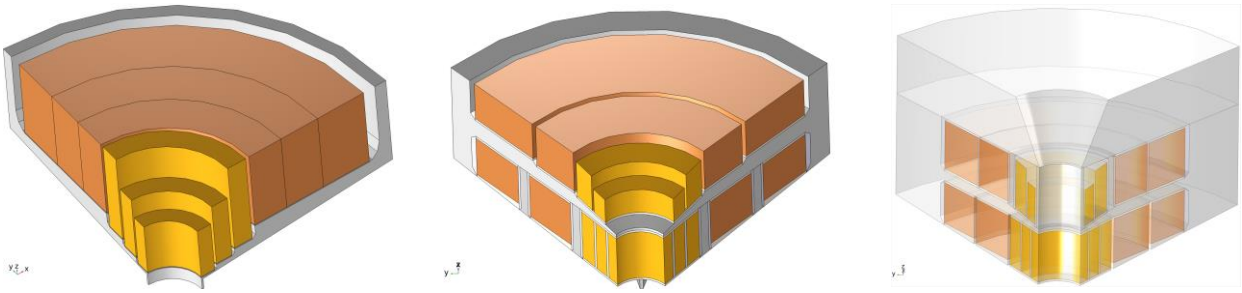

Fig. 3a-c. Views from above a quadrant of the upper half of illustrative magnets to meet the specs of Table I. Gold-colored is ReBCO tape; copper-colored is low-temperature superconductor (LTS); grey is support-structure material, likely stainless steel. Left: Coils supported by platen near magnet midplane. Center: Outboard coils supported by platen bearing on rings resting on midplane pie wedges. Right: Platen supported by rings extending downward from thick outboard cantilever.

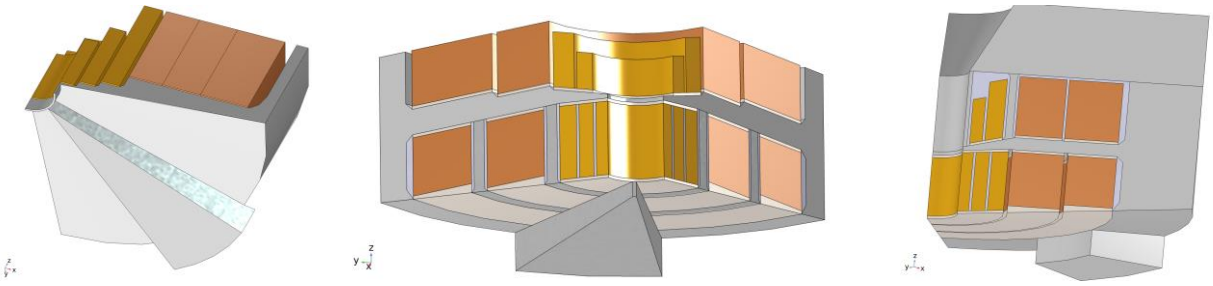

Fig. 4a-c. Views from below a quadrant of the upper half of the illustrative magnets of Fig. 3. Below each quadrant is pie wedge (blunt-nosed in 4c), flaring axially by 5° and circumferentially by ~30°, that bears the cross-midplane force of attraction between the coils above and below the magnet midplane

Figures 3a and 4a show a geometry in which coils bear on a platen near the magnet midplane, which in turn bears on pie wedges to carry across the magnet midplane the enormous force with which one half magnet attracts its mate across the magnet midplane. Bridging the circumferential spans between the wedges is a platen postulated to have the strength and stiffness of stainless steel. Stiffer alternatives could reduce deformations to less than half; candidates to consider are tungsten, molybdenum, or steels stiffened by large percentages of titanium diboride. Circumferentially between the pie wedge and an identical one in an adjacent quadrant is the port—ideally flaring as broadly as feasible both axially and circumferentially—that allows scattered neutrons to reach detectors without traversing material other than cryostat walls.

Figures 3b and 4b show a design in which the platen is much further from the magnet midplane, thereby displacing conductor that is much less efficient at generating magnetic field. Supporting the platen are rings interpolated radially between selected inboard coils to carry the magnetic force with which the outboard coils are attracted downward by the other coils. The inboard coils need no mechanical support, because they are attracted more strongly upward by the outboard coils than downward by the coils across the midplane.

Figures 3c and 4c show a design that threads the load-bearing rings between radial gaps between outboard coils rather than inboard ones, moving the displaced conductor to a region of even lower field-generating efficiency. The rings, now in axial tension rather than compression, hang from a thick outboard platen cantilevered from a comparably-thick ring radially beyond all of the magnets. Because the cross-midplane support is now at such a large radius, it need block only a small fraction of the available circumference.

Geometry with Coils Support very near Midplane of Magnet

The magnet of Fig. 3a/4a uses 1.89 litres of ReBCO, 11.96 liters of Nb_3Sn, and 8.72 liters of stainless steel. Figure 5 plots its field magnitude; the maximum field is 29.16 T; that seen by the Nb_3Sn is 14 T. The total magnetic energy of the magnet is 1.42 MJ. The axial magnetic force of attraction between the two magnet halves is 3.29 MN.

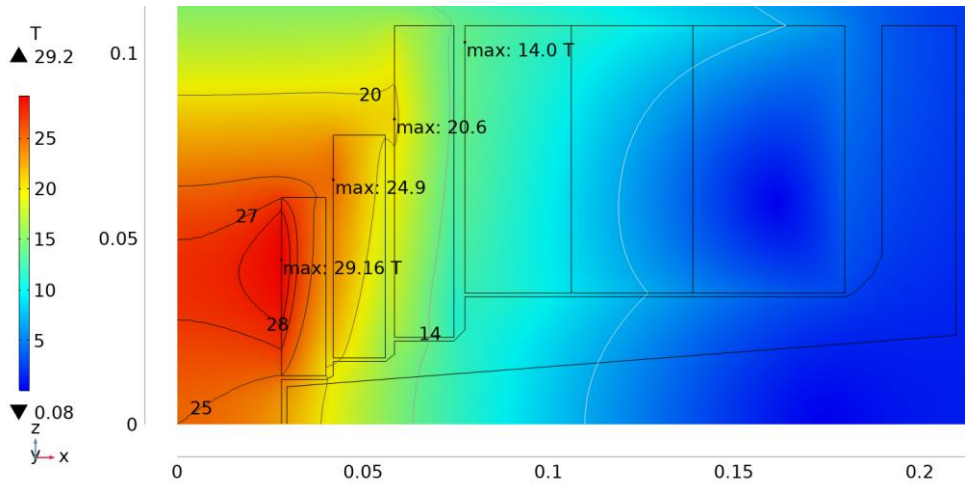

Fig. 5. Field magnitude of magnet of Fig. 3a & 4a. The maximum ambient field is 29.2 T; that seen by the Nb_3Sn is 14 T. Tesla contours are 7, 14, 20, 25, 27 and 28. The total magnetic energy of the magnet is 1.41 MJ. The axial magnetic force of attraction between the two magnet halves is 3.29 MN.

Figures 6 and 7 plot the von Mises stress and first principal strain in this illustrative magnet.

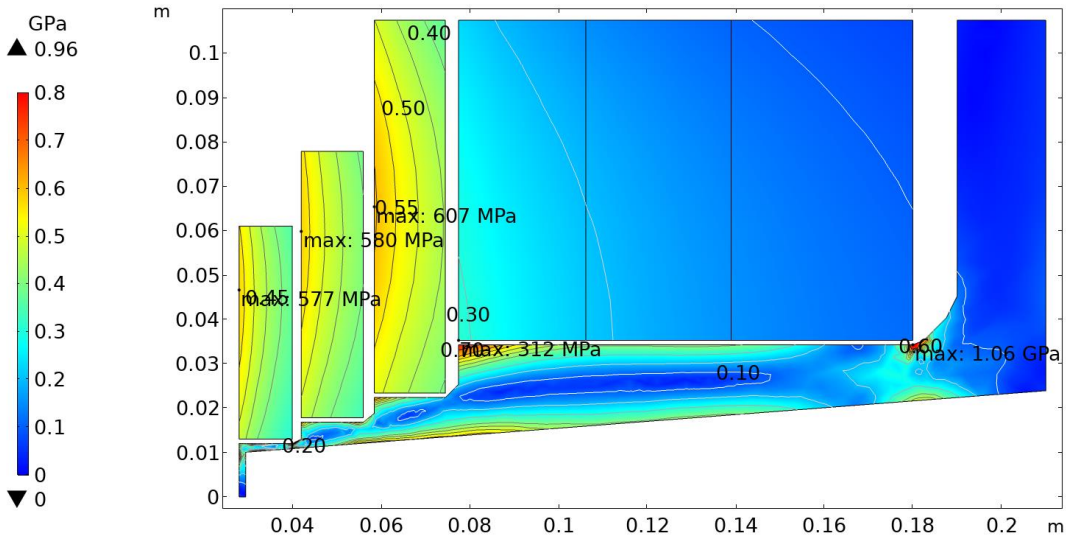

Fig. 6. Von Mises stress σ_{vM} in magnet of Fig. 5. The maximum von Mises stress in each of the three ReBCO coils is approximately 600 MPa, the maximum recommended for the conductor; σ_{vM} in the Nb_3Sn reaches 312 MPa. In the support material the maximum stress, 1.06 GPa, may be sufficiently localized to be acceptable.

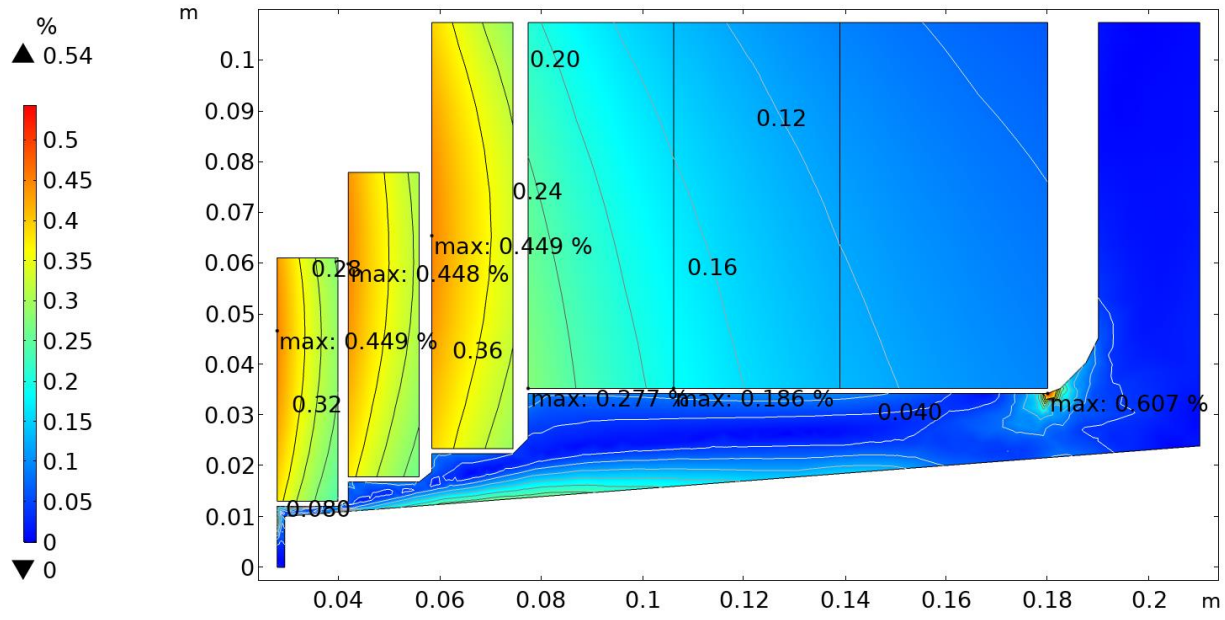

Fig. 7. First principal strain ε_1 in magnet of Figs. 5 & 6. The maximum strain in each of the three ReBCO coils is 0.45%, the maximum recommended for the conductor; ε_1 in the Nb_3Sn reaches 0.277%. In the support material the maximum strain, 0.61%, may be sufficiently localized to be acceptable.

Technical Objectives: Concept of Revolutionary, Open-Midplane Design of Magnet

The revolutionary designs whose development this SBIR/STTR advanced employ magnetic attraction instead of mechanical support for the inner solenoids of a magnet with multiple nested split-solenoids—i.e., solenoids with a midplane gap, as in a Helmholtz pair. Coils that are outboard (i.e., relatively far from the magnet midplane) magnetically attract inboard coils so strongly as to overpower the attractive force from coils on the opposite side of the magnet midplane. These inner coils therefore need no midplane-straddling structure for mechanical support. Support for the outboard coils straddles the midplane, but only through pie wedges confined to circumferential regions that are at least ±30° from the axis of the viewing port. Inspiration for the design was the "open-midplane dipole" design[11,12] proposed nearly two decades ago by Ramesh Gupta and pioneered by a collaboration of PBL and BNL.[13]

To increase viewing port angles and magnet efficiency, coils ideally have a cross section that is not a rectangle but a parallelogram, with its inboard edge paralleling the flare angle of the magnet's midplane viewing port. Wherever the field is too intense for low-temperature superconductors, the conductor is ReBCO tape, assumed 12 mm wide, wound into pancakes that are dished slightly into a very blunt cone, like a nearly flat cone spring. Figure 8 illustrates this key component to improve magnet efficiency and field homogeneity. A task completed by this SBIR was the winding of such coils and testing them, not only at 77 K, as originally proposed, but also at 4 K.

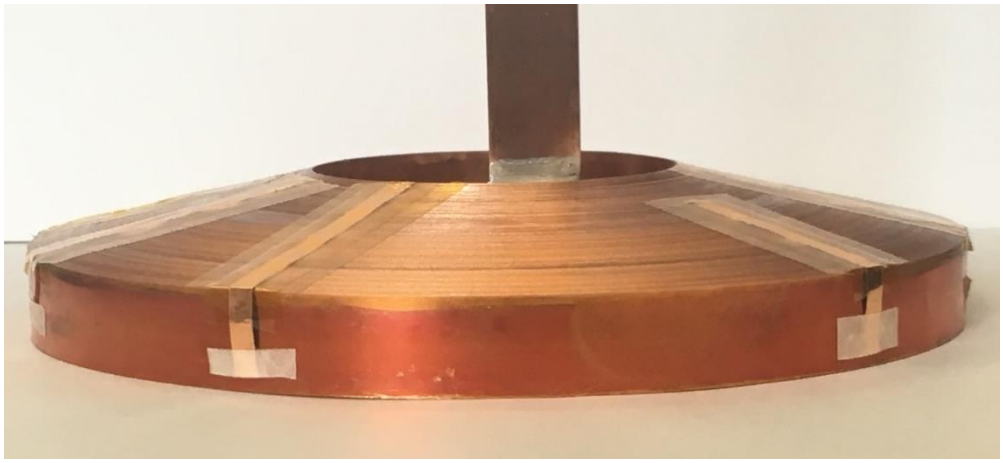

Fig. 8. Conical coil of 315 turns (88 m) of ReBCO tape 12 mm wide and 0.12 mm thick, wound by the BNL Superconducting Magnet Division. I.D. = 51 mm; O.D. = 127 mm; cone angle = 15°; cone height = 10 mm.

Design with Magnetic Support of Inboard Coils, Platen Support of Outboard Coils

The magnet of Figs. 3b/4b uses 1.45 liters of ReBCO, 8.17 liters of Nb_3Sn, 3.28 liters of NbTi, and 8.88 liters of support structure. Its estimated material cost is only 70% that of the previous design.

Figure 9 plots the magnetic field intensity throughout the magnet. Coil dimensions attempt to minimize the use of expensive HTS, substituting Nb_3Sn or NbTi wherever the ambient field is not too intense.

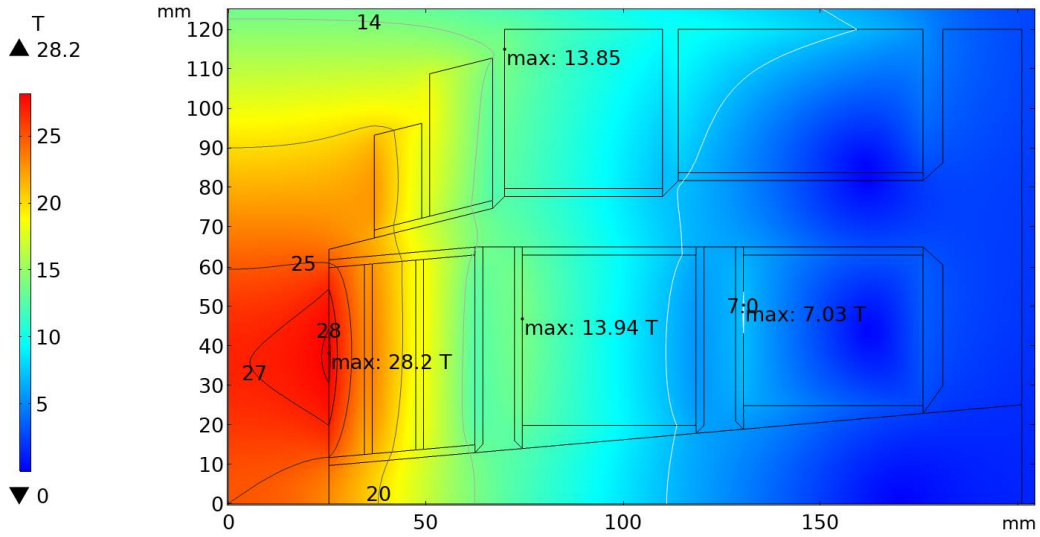

Fig. 9. Geometry and ambient field magnitude B. The midplane cone angle is ±5°; axial access is ±18°). B_{max} in the ReBCO tape is 28.2 T; selected contours suggest where Nb_3Sn or NbTi suffices instead of HTS: 14 T for Nb_3Sn and 7 T for NbTi. The magnetic energy, U_m, is 1.28 MJ; the attraction between the magnet halves is 3.27 MN.

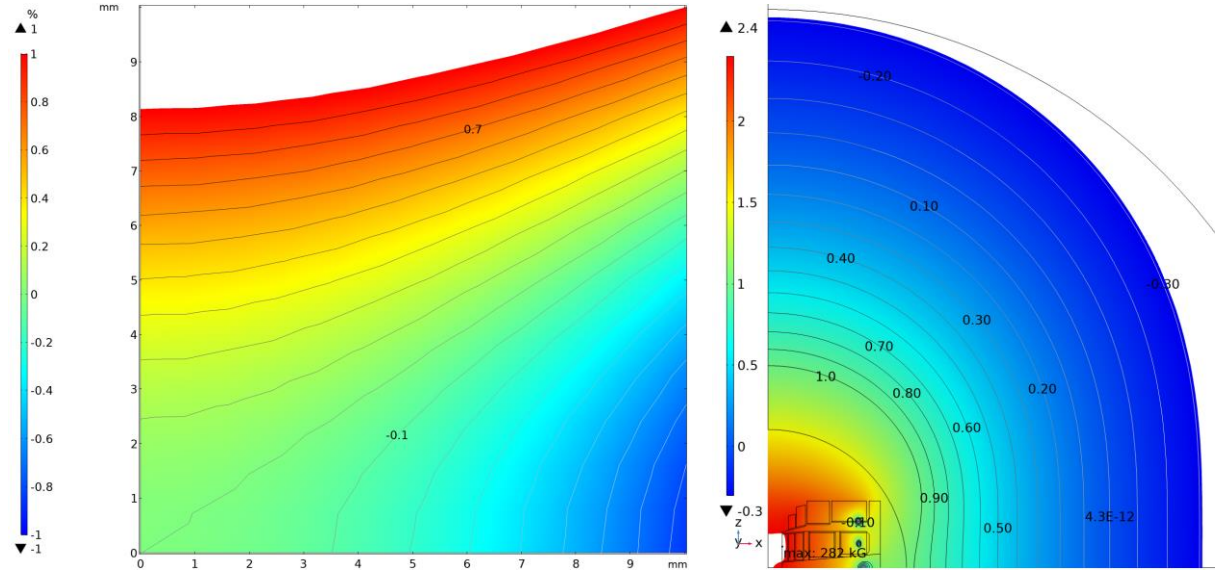

Fig. 10a&b. Field homogeneity and fringe field. Left: The peak-to-peak field inhomogeneity is 1.44% over a cylinder of 7.5 mm radius and half-length. Right: log10|B[kG]|. The successive kG contours are [$10^{-0.3}$=0.5, 0.64, 0.8, 1.0, 1.25, 1.6, 2, 2.5, 3.2, 4.0, 5.0, 6.4, 8.0, 10]. On-axis the blue-to-white border ($10^{-0.3} \approx 0.5$ kG) nearly reaches the black arc, r = 1 m; extrapolating $B \sim r^{-3}$ predicts a field less than half the allowed 0.1 kG at 2 m.

Figure 11 plots $|F_z|$, the absolute value of the density of the component of Lorentz force parallel to the axis of the magnet, facilitating comparison of the upward and downward forces by showing equal magnitudes as equal colors. Throughout the white band within each coil $|F_z|$ is less than 0.2 N/mm^3. Above the band, forces are downwards, toward the magnet midplane; below the band, they are upwards. The net force, in kN, on each of the five successive inboard coils is 0.67, 5.1, 11, 28 and 5.6—all upwards, as intended. The downward force on successive outboard coils is 84, 303, 862 and 2069 kN. The total downward force is 3.27 MN.

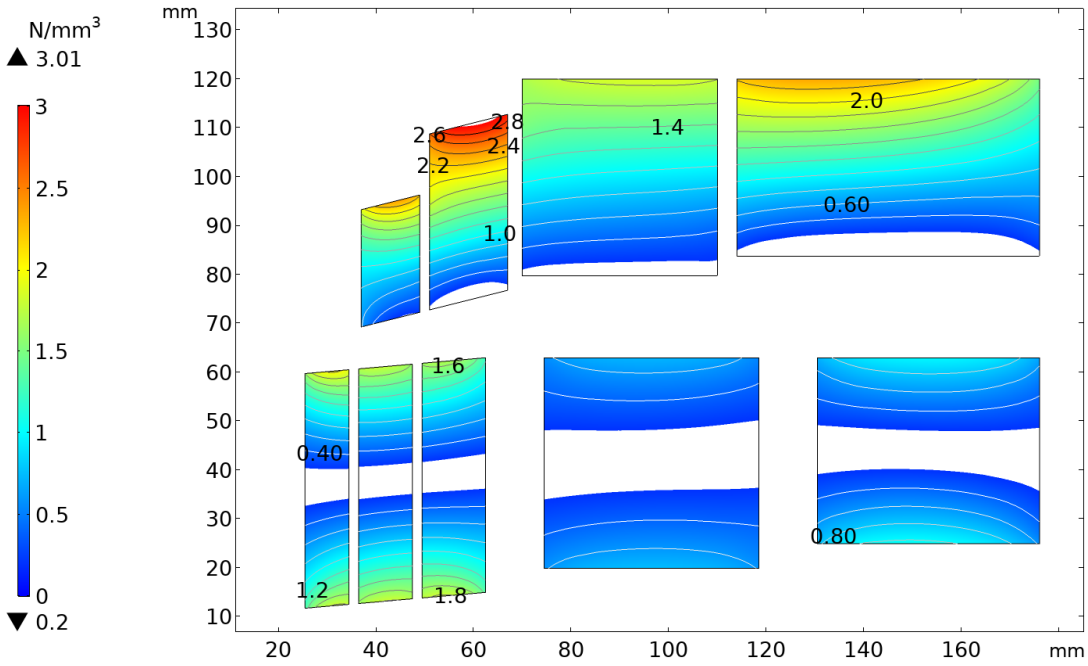

Fig. 11. Absolute value of axial Lorentz force density in magnet of Fig. 9. Magnetic attraction from outboard coils attracts inboard coils upward, overpowering the downward attraction from coils on the opposite side of the midplane. Within the white band, $|F_z| < 0.2$ N/mm^3. Axially outboard of the band, F_z is toward the magnet midplane; axially inboard, it is away. The net force on each inboard coil is away from the midplane.

Figures 12&13 plots the vertical displacement of coils and platen. The coils are postulated to be orthotropic, with circumferential, axial and radial Young's moduli of [150, 120, 30] for ReBCO and [100, 20, 20] for bothNb_3Sn and NbTi. The support structure is isotropic, postulated to have the Young's modulus of molybdenum: 312 GPa. With such a stiff support material, the maximum displacement is only 0.28 mm in the platen and 0.35 mm in the conductor.

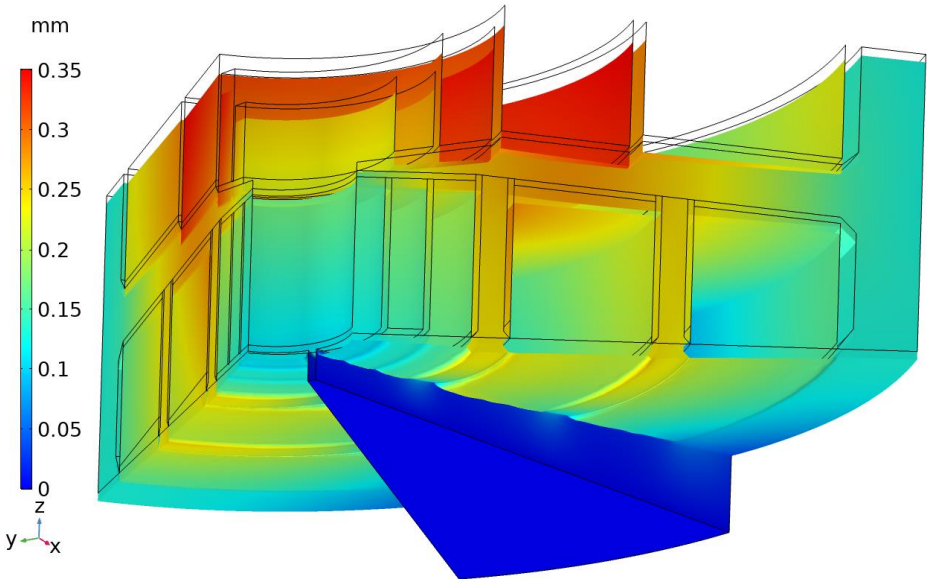

Fig, 12. Axial displacements δ_z, magnified twentyfold.

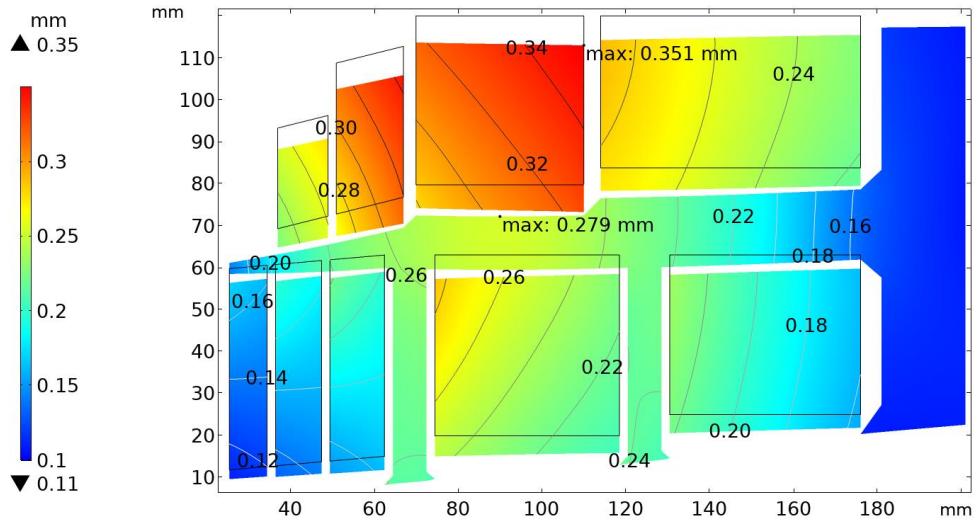

Fig. 13. Axial displacements δ_z at mid-span between pie wedges, magnified twenty-fold. The maximum δ_z is 0.28 mm in the platen and 0.35 mm in the coils.

Figure 14 plots the von Mises stress in the coils and support structure. In each of the ReBCO coils the von Mises stress is very nearly 500 MPa, a comfortable margin less than the 600 MPa maximum recommended for the conductor.

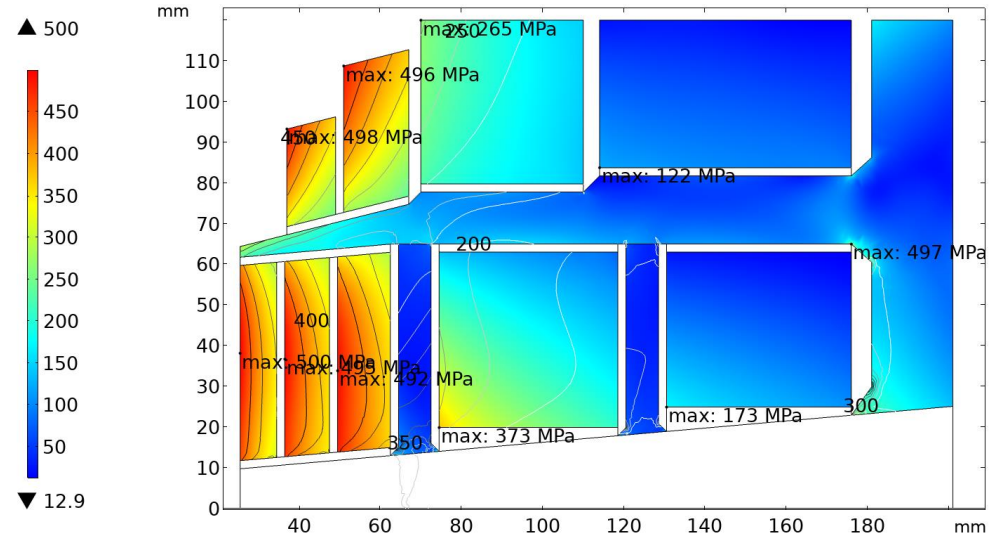

Fig. 14. Von Mises stress, σ_{vM}. At the mid-span between pie wedges, the maximum σ_{vM} is 497 MPa in the platen, 173 MPa in the NbTi coil, and ranges from 122 MPa to 373 MPa in the Nb_3Sn coils and 492 MPa to 500 MPa in the ReBCO coils.

Figure 15 plots the first principal strain in the coils. In the ReBCO coils, it never exceeds 0.387%, a margin of 16% to the 0.45% maximum recommended for the conductor. In the NbTi coil, the maximum strain is only 0.156%; in the Nb_3Sn coils the range is from 0.104% to 0.338%. The platen maximum is 0.474%.

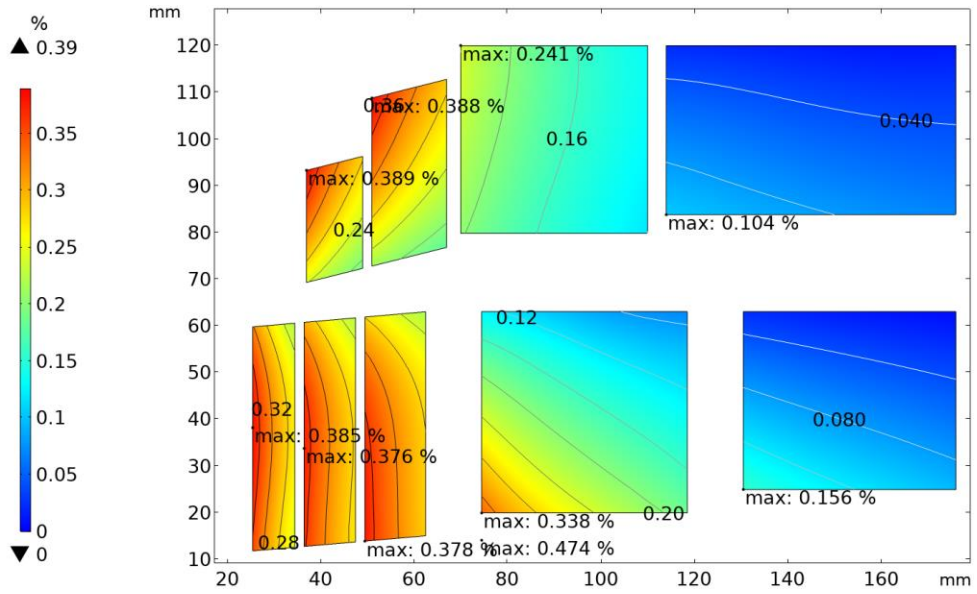

Fig. 15. First principal strain ε_1. At the mid-span between pie wedges, the maximum ε_1 is 0.474% in the platen, 0.156% in the NbTi coil, and ranges from 0.104% to 0.338% in the Nb_3Sn coils and 0.376% to 0.389% in the ReBCO coils.

Figure 16a&b reveals stress concentrations where the support rings bear against the pie wedges. These may be sufficiently localized to be acceptable. If not, gently crowning the pie wedge and/or support rings should spread the load to reduce the stress concentrations.

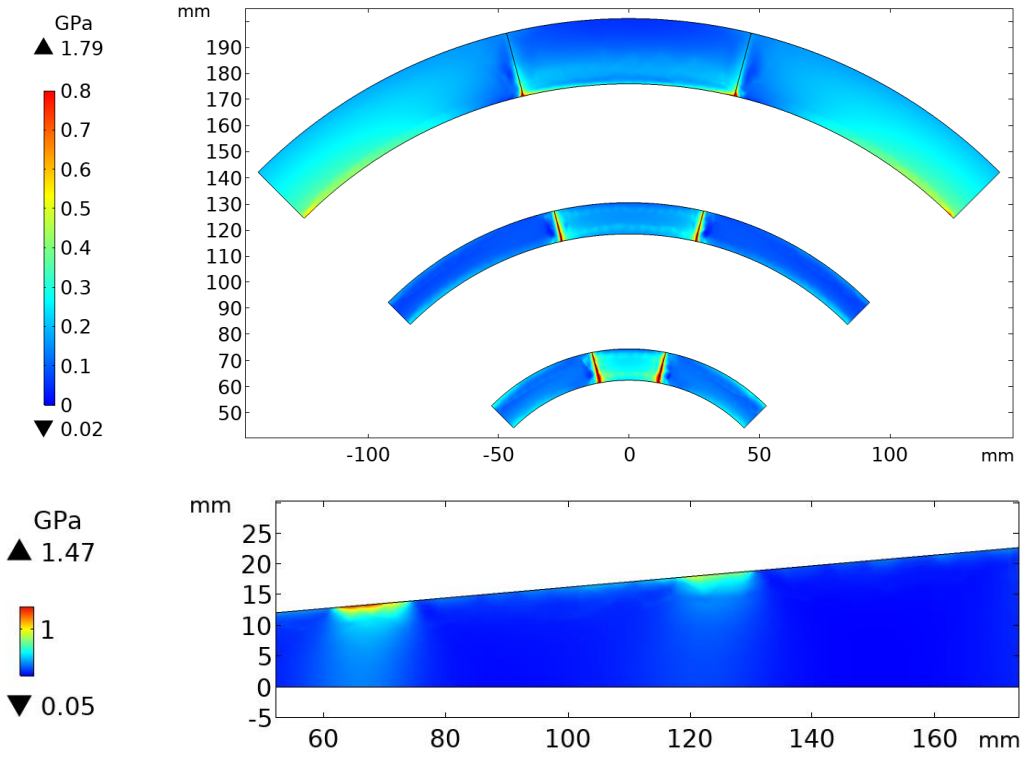

Fig, 16a&b. Localized von Mises stress concentrations where the support rings bear on the pie wedges. Top: Inboard side of support rings. Bottom: Typical radial/axial face of pie wedge.

Design with Magnetic Support of Inboard Coils, Cantilever Support of Outboard Coils

Magnet 3c/4c uses 1.49 liters of ReBCO, 7.42 liters of Nb_3Sn, 2.63 liters of NbTi, and 33.2 liters of support structure. Its estimated material cost is 78% that of design 3a/4a.

Figure 17 plots the field magnitude in a magnet of the geometry of Figs. 3c/4c, in which support of the outboard coils is from a robust cantilever supported by a comparably robust ring radially outside the coils. The maximum ambient field coincidentally is the same 28.2 T as in Fig. 9.

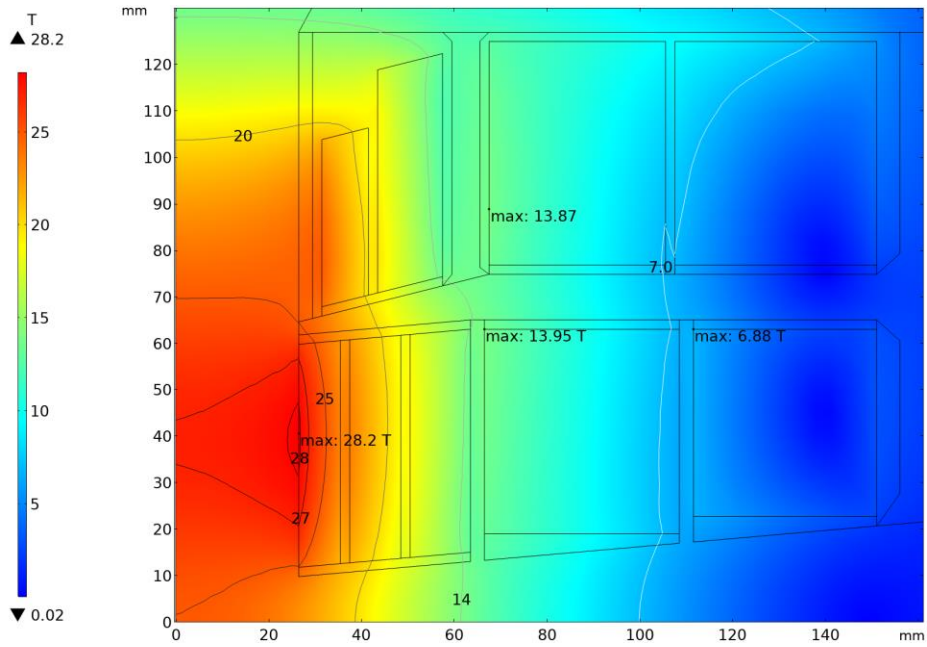

Fig. 17. Ambient field magnitude B for the magnet of Figs. 3c/4c. B_{max} in the ReBCO tape is 28.2 T; selected contours suggest where Nb_3Sn or NbTi suffices instead of HTS: 14 T for Nb_3Sn and 7 T for NbTi. The magnetic energy, U_m, is 1.104 MJ.

Figure 18a&b plots the field homogeneity and fringe field of the magnet of Fig. 17.

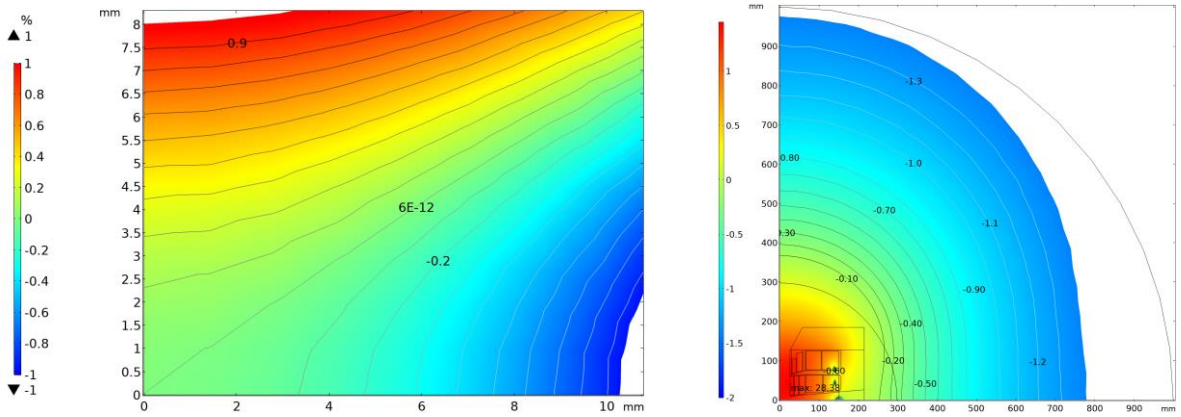

Fig. 18a&b. Field homogeneity and fringe field. Left: The field homogeneity is 1.32% over a cylinder of 7.5 mm radius and half-length. Right: log10|B[kG]|. The successive kG contours are [$10^{-0.3}$=0.5, 0.64, 0.8, 1.0, 1.25, 1.6, 2, 2.5, 3.2, 4.0, 5.0, 6.4, 8.0, 10]. On-axis the blue-to-white border ($10^{-0.4} \approx 0.4$ kG) nearly reaches the black arc, r = 1 m; extrapolating $B \sim r^{-3}$ predicts a field less than half the allowed 0.1 kG at 2 m.

Figure 19 plots $|F_z|$, the absolute value of the density of the component of Lorentz force parallel to the axis of the magnet, facilitating comparison of the upward and downward forces by showing equal magnitudes as equal colors. Throughout the white band within each coil $|F_z|$ is less than 0.2 N/mm^3. Above the band, forces are downwards, toward the magnet midplane; below the band, they are upwards. The net upward force, in kN, on each of the five successive inboard coils is 3.1, 5.4, 7.0, 18.3 and 27.1; the downward forces on each of the four successive outboard coils is 23, 92, 239 and 424.

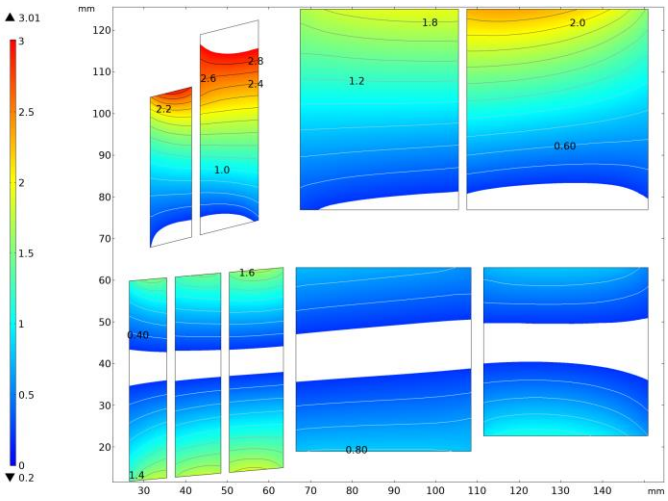

Fig. 19. Absolute value of density of axial Lorentz force in magnet of Fig. 17. Magnetic attraction from outboard coils attracts inboard coils upward, overpowering the downward attraction from coils on the opposite side of the midplane. Within the white band, $|F_z| < 0.2$ N/mm^3. Axially outboard of the band F_z is toward the magnet midplane; axially inboard, it is away from the midplane. The net force on each inboard coil is away from the midplane.

Figure 20a&b plots the axial displacement with a support structure with a Young's modulus of 208 GPa. With a support structure this massive, its maximum axial displacement is a mere 0.44 mm; that in the conductor is very little more: 0.53 mm.

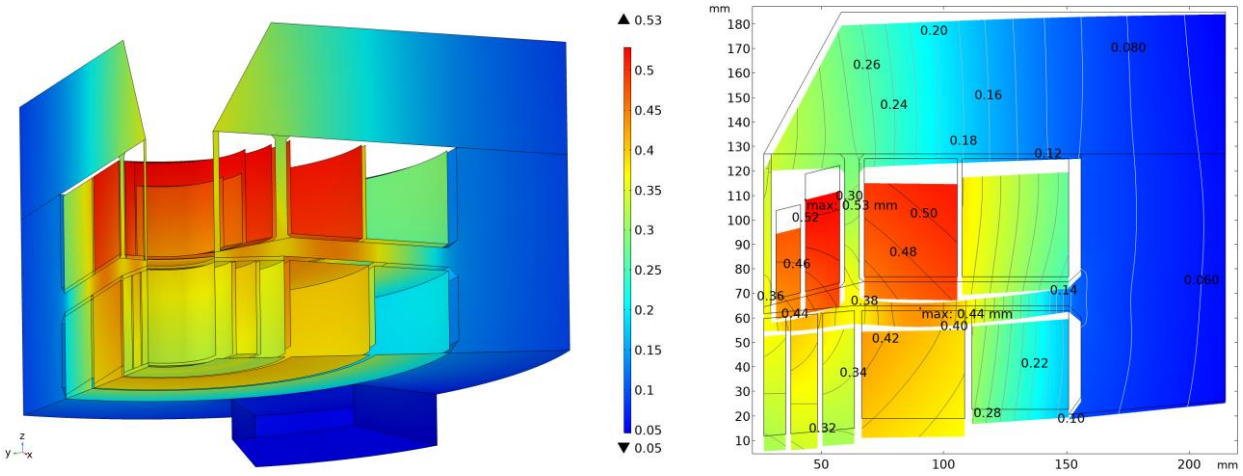

Fig. 20a&b. Axial displacements δ_z , magnified twenty-fold. Left: 3-D. Right: At mid-span between pie wedges. The maximum δ_z is 0.53 mm in the coils and 0.44 mm in the intra-coil platen.

Figure 21 plots the von Mises stress. In all five ReBCO coils it is just shy of 500 MPa, providing a 20% margin to the 600 MPa maximum recommended for the conductor. The more than 1 GPa stress concentration at corners between the platen and rings may be so localized to be acceptable.

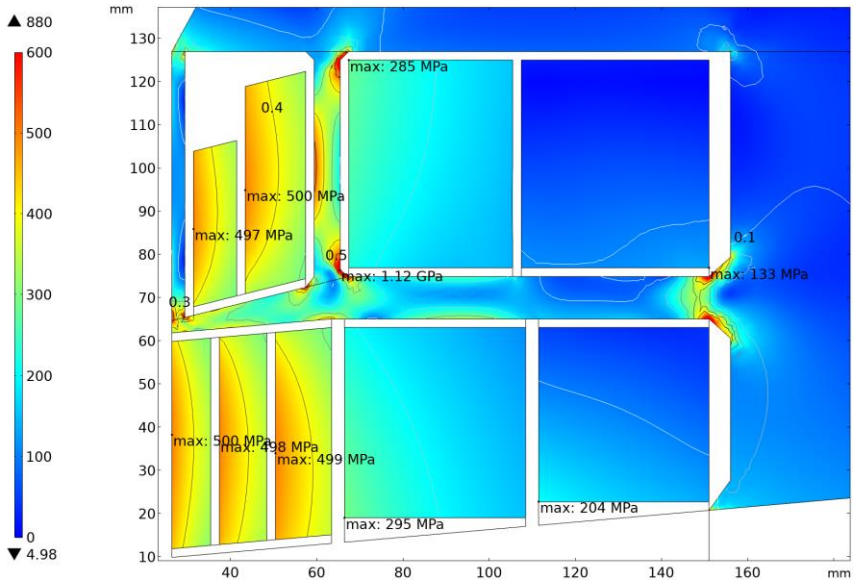

Fig. 21. Von Mises stress, σ_{vM}. In all five of the ReBCO coils the maximum von Mises stress is very nearly 500 MPa; in the NbTi it is 204 MPa; in the Nb_3Sn, it ranges from 133 MPa to 295 MPa.

Figure 22 plots the first principal strain, ε_1. In each ReBCO coil, ε_1 is approximately 0.38 %, providing a nearly 20% margin to the 0.45% maximum recommended for ReBCO.

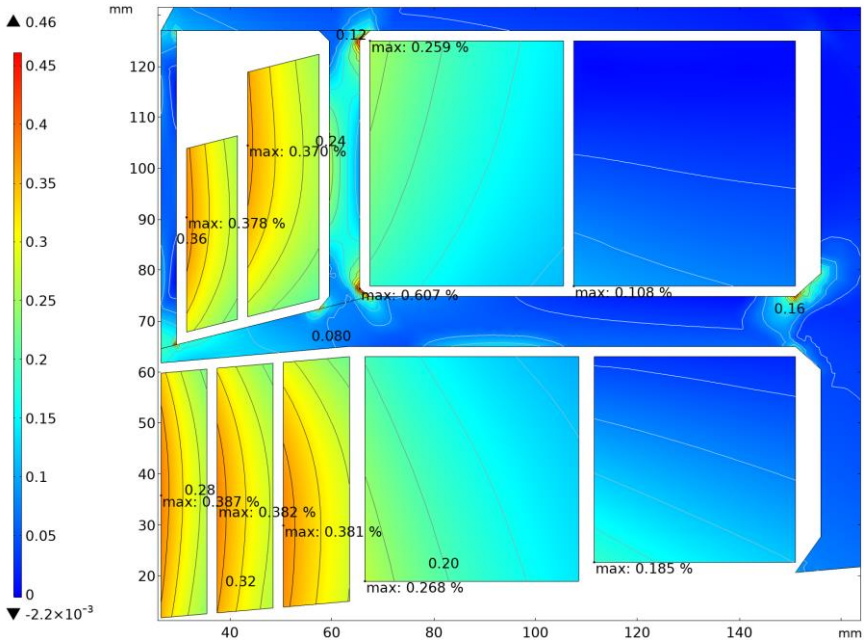

Fig. 22. First principal strain ε_1. In all five ReBCO coils the maximum ε_1 is less than 0.4%; in the NbTi coil it is 0.185%; in the Nb_3Sn coils it ranges from 0.108% to 0.268%. In the platen, it reaches as much as 0.607%, but over so small a region as perhaps to be acceptable.

Figure 23 plots the von Mises stress concentrations where the pie wedge supports the outermost ring. The maximum von Mises stress reaches only 0.79 GPa in the ring and 644 MPa in the pie wedge.

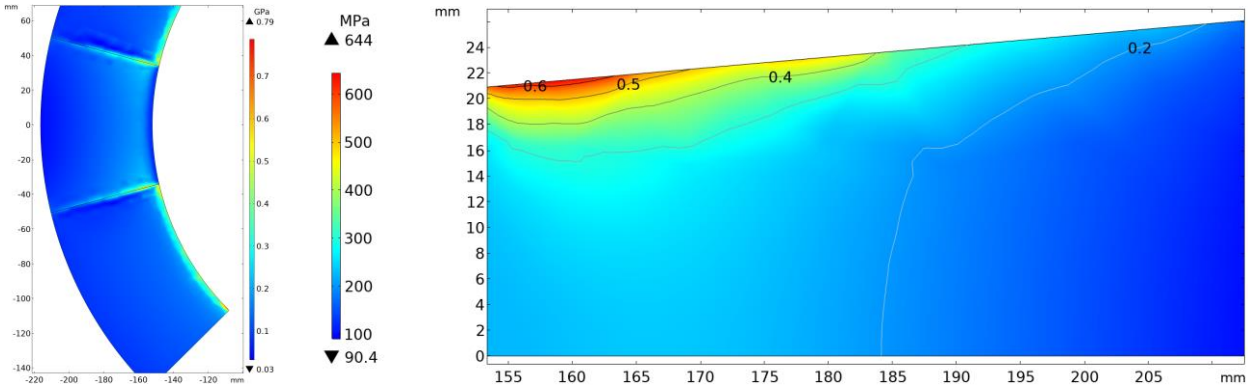

Fig, 23a&b. Localized von Mises stress concentrations where the support rings bear on the pie wedges. Left: Top of pie wedge. Right: Circumferential face of pie wedge.

References

1. Nat. Res. Council, "High Magnetic Field Science and Its Application in the United States: Current Status and Future Directions," Washington, DC, Nat. Acad. Press. https://www.nap.edu/read/18355, ISBN 0309387787, 9780309387781 (2013) doi: https://doi.org/10.17226/18355.
2. Workshop on Probing Matter with X-Rays and Neutrons at the National High Magnetic Field Laboratory, Tallahassee, FL, May 10-12, 2005.
3. B. Winn, M.B. Stone, et al., Workshop on Neutron Scattering and High Mag. Fields, Sept. 4-5, 2013, https://neutrons.ornl.gov/sites/default/files/WorkshopReportFINAL_FINAL.pdf. ORNL/TM-2014/652, doi: 10.2172/1410956 (2014).
4. B. Winn, et al. Tech. Report: Ultra-High Field Magnets for X-Ray and Neutron Scattering using High Temperature Superconductors, https://info.ornl.gov/sites/publications/Files/Pub71968.pdf. ORNL/TM-2016/712, DOI: 10.2172/1432171 (2017).
5. O. Prokhnenko, et al. Time-of-flight Extreme Environment Diffractometer at the Helmholtz-Zentrum Berlin. Rev. Sci. Instr. **86**, 033102 (2015); doi: 10.1063/1.4913656.
6. HFM/EXED. High Magnetic Field Facility for Neutron Scattering. https://www.helmholtz-berlin.de/pubbin/igama_output?modus=einzel&gid=1939&sprache=en.
7. F.J. Brown, J. Phys.: Conf. Ser. **251**, 012093 (2010).
8. R.B.E. Down, et al., J. Phys.: Conf. Ser. **251** 012092 (2010).
9. O. Kirichek, et al., J. Phys.: Conf. Ser. **400** 052013 (2012).
10. A.T. Holmes, et al., Rev. Sci. Instr. **83**, 023904 (2012); doi: 10.1063/1.3688657.
11. T. Panesor & E. Woodfield, "Neutron scattering," Institute of Physics 2010, https://www.iop.org/publications/iop/2011/file_47455.pdf
12. R. Gupta, et al., "Open-Midplane Dipole Design for LHC IR Upgrade," MT18, Morioka City, Japan (2003).
13. R. Gupta, et al., "Optimization of Open Midplane Dipole Design for LHC IR Upgrade," PAC'05, Knoxville, TN, USA (2005).
14. R. Weggel, et al., "Open-Midplane Dipoles for a Muon Collider," PAC11, NY, NY (2011); BNL-95145-2011-CP.
15. R. Gupta, et al., "High Field HTS R&D Solenoid for Muon Collider," presented at 2010 Applied Superconductivity Conf., Trans. on Appl. Supercond.
16. R. Weggel, et al., "An ongoing study to test a YBCO HTS magnet at fields approaching 40 T," Neutron Factory and Muon Collider Collaboration-DOC-553, 2010.
17. Y. Shiroyanagi, R. Gupta, P. Joshi, H. Kirk, R. Palmer, W. Sampson, P. Wanderer, D. Cline, A. Garren, J. Kolonko R. Scanlan, R. Weggel, "15+ T HTS Solenoid for Muon Accelerator Program," 3rd Int. Particle Acc. Conf. (IPAC 2012).